



# EI-Lite: Electrical Impedance Sensing for Micro-gesture Recognition and Pinch Force Estimation

Junyi Zhu University of Michigan Ann Arbor, MI, USA zhujunyi@umich.edu	Tianyu Xu Google Mountain View, CA, USA tyx@google.com	Jiayu Wang University of Washington Seattle, WA, USA jiayuw4@uw.edu	Emily Guan Pratt Institute Brooklyn, NY, USA eguan12@pratt.edu
JaeYoung Moon GIST Gwangju, Republic of Korea super_moon@gm.gist.ac.kr	Stiven Morvan Google New York, NY, USA mstiven@google.com	D Shin Google Mountain View, CA, USA deshin@google.com	Andrea Colaço Google Mountain View, CA, USA andreacolaco@google.com
Stefanie Mueller MIT CSAIL Cambridge, MA, USA stefanie.mueller@mit.edu	Karan Ahuja Northwestern University Evanston, IL, USA kahuja@northwestern.edu	Yiyue Luo University of Washington Seattle, WA, USA yiueluo@uw.edu	Ishan Chatterjee Google Seattle, WA, USA ishanc@google.com

**Figure 1: EI-Lite is a lightweight electrical impedance sensing system for (a) micro-gesture recognition and (b) continuous pinch force estimation. (c) Application scenarios demonstrate EI-Lite’s usage as an input interface for assistive technologies, interactive systems, and AR/VR experiences.**

## Abstract

Micro-gesture recognition and fine-grain pinch press enables intuitive and discreet control of devices, offering significant potential for enhancing human-computer interaction (HCI). In this paper, we present EI-Lite, a lightweight wrist-worn electrical impedance sensing device for micro-gesture recognition and continuous pinch force estimation. We elicit an optimal and simplified device architecture through an ablation study on electrode placement with 13 users, and implement the elicited designs through 3D printing. We capture data on 15 participants on (1) six common micro-gestures (plus idle state) and (2) index finger pinch forces, then develop machine learning models that interpret the impedance signals generated by these micro-gestures and pinch forces. Our system is capable of accurate recognition of micro-gesture events (96.33%

accuracy), as well as continuously estimating the pinch force of the index finger in physical units (Newton), with the mean-squared-error (MSE) of 0.3071 (or mean-force-variance of 0.55 Newtons) over 15 participants. Finally, we demonstrate EI-Lite’s applicability via three applications in AR/VR, gaming, and assistive technologies.

## CCS Concepts

- Human-centered computing → Human computer interaction (HCI).

## Keywords

Micro-gesture Recognition, Input, Natural User Interfaces, Interaction Technique, Extended Reality, EIT

## ACM Reference Format:

Junyi Zhu, Tianyu Xu, Jiayu Wang, Emily Guan, JaeYoung Moon, Stiven Morvan, D Shin, Andrea Colaço, Stefanie Mueller, Karan Ahuja, Yiyue Luo, and Ishan Chatterjee. 2025. EI-Lite: Electrical Impedance Sensing for Micro-gesture Recognition and Pinch Force Estimation. In *The 38th Annual ACM Symposium on User Interface Software and Technology (UIST ’25)*, September 28–October 01, 2025, Busan, Republic of Korea. ACM, New York, NY, USA, 14 pages. <https://doi.org/10.1145/3746059.3747671>



This work is licensed under a Creative Commons Attribution 4.0 International License.  
*UIST ’25, Busan, Republic of Korea*  
 © 2025 Copyright held by the owner/author(s).  
 ACM ISBN 979-8-4007-2037-6/25/09  
<https://doi.org/10.1145/3746059.3747671>

## 1 Introduction

Micro-gestures and pinch forces are subtle and often imperceptible hand movements. They are widely applied in scenarios where conventional input methods are impractical or intrusive, playing a crucial role in human-computer interaction [34, 46], augmented/virtual reality (AR/VR) [22, 27], and assistive technologies [5, 45]. The discreet and ergonomic nature of micro-gestures make them very compelling for simple 1-D and 2-D mobile UI control, such as those found on smartwatches [1, 38], earbuds, or smartglasses [43]. However, micro-gestures and continuous pinch forces are inherently difficult to capture due to their mechanically subtle nature. Previous work has explored capturing them using cameras [29, 35], which, while effective, limits the ubiquity of sensing due to power and privacy in mobile contexts. Practical micro-gesture recognition and pinch force estimation require a wearable setup that balances comfort, usability, simplicity, and precision.

Electrical impedance sensing emerges as a promising technology for subtle and imperceptible hand movements because of its simple, compact sensor design, and noise-resistant active sensing mechanism. This approach takes pairwise active impedance measurements from surface electrodes, which enables reconstruction of internal impedance variations [15]. It has been widely applied for non-invasive and low-cost medical imaging [7, 13]. In the past years, wearable electrical impedance sensing devices have been explored for diverse applications in human-computer interaction, including gesture classification [24, 59, 61], activity detection [39], and rehabilitation [63]. Despite these advances, challenges remain in minor hand movement detection via electrical impedance sensing. Unlike full hand gestures, micro-gestures and pinch forces are much more subtle, producing minimal activity in the tendons and muscles and leading to weak signals that are difficult for electrical impedance sensors to detect. Furthermore, the complex anatomical structures of the wrist (from the radioulnar joint to the proximal carpal row) [11] introduce significant variations in electrical impedance sensing performance. These variations not only differ significantly among users but also depend heavily on electrode placement around the wrist. Additionally, to ensure the comfort and usability of a wrist-worn device and to build toward a system that can be practically realized for mobile use, the number of electrodes should be minimized without compromising system performance for those applications, and enable high sensing FPS required for micro-gesture detection.

Towards this goal of enabling lightweight, mobile UI control, we introduce EI-Lite, a practical and efficient approach for micro-gesture recognition and continuous pinch force estimation using an optimized wrist-worn electrical impedance sensing device. To overcome the challenges of impedance signal variances due to complex anatomical structures, we first identify the optimal placement of electrodes by conducting a user study with 13 participants, which captures electrical impedance signals from  $32 \times 2$  sensing electrodes covering both the proximal carpal row and the distal radioulnar joint areas around the wrist. We further perform an electrode ablation evaluation to determine which sensor locations provide the greatest discriminatory information for microgesture sensing across users. From this information, we implement EI-Lite, an electrical impedance sensing wristband with only 4 electrodes (the minimum

number of electrodes for a 4-terminal impedance measurement), and a custom impedance sensing board for retrieval of 6 cross-pair readings (all possible 4-terminal measurement combinations with 4 electrodes) at 100Hz. As finger movements during microgestures and forced pinch are extremely subtle, our customized impedance sensing board captures both real (magnitude) and imaginary (phase) components of bio-impedance, moving beyond previous approaches that utilize only real values. Compared to the previous electrical impedance sensing approaches for full hand gestures, which primarily look at only the real part of the impedance signals, we implemented a customized impedance sensing board that is capable of accurate imaginary part sensing as well, to accommodate the subtle and imperceptible finger movements during micro-gesture and pinch pressing. Thus EI-Lite is not only the first wrist-worn bioimpedance system to robustly sense such subtle micro-gestures and pinch forces, but also does so using a minimal number of electrodes, enhancing user comfort by reducing device obtrusiveness, and moving one step closer toward a practically realizable system.

We leverage EI-Lite for micro-gesture recognition and pinch force estimation coupling with machine learning models and few-shots learning techniques. We collect two datasets over 15 participants featuring 6 common micro-gestures plus idle state, and continuous pinching forces. Towards the goal of mobile UI control, our gestures set include both selection as well as scrolling type gestures. Due to familiarity with touchscreen interactions, both finger pinches and thumb swipes have been cited as comfortable and intuitive in micro-gesture design and elicitation studies [3, 17]. Thus, our gesture set targets taps and swipes, specifically: index finger pinch, index finger pinch release, middle finger pinch, middle finger pinch release, swipe left, and swipe right, as shown in Figure 1a. This gesture set also demonstrates some of the capabilities possible with electroimpedance, but not with IMU-based techniques, including stateful pinch and directional swiping. The pinch force dataset contains impedance continuous index pinch forces measured in Newtons (Figure 1b). We demonstrate micro-gesture classification with the accuracy of 96.33% and continuous estimation of index pinch forces (in Newton) with the mean square error of 0.3071 (or mean force variance of 0.55 Newtons). To further address the challenges of impedance signal variances across users, we explore few-shot learning framework for the generalization of our model. To evaluate the practicality of our system, we implement three application examples (Figure 1c): (1) hand movements input for XR headset while outside of the camera's field-of-view, and pressing force input for XR environment, (2) seamless and subtle interaction control for daily activities such as teaching presentations, and (3) assistive smart watch input for users with limited hand functions.

In summary, we contribute the following:

- an ablation study with 13 participants to identify optimal impedance sensing locations and electrode configurations for micro-gesture recognition around the wrist
- the development of the EI-Lite system, featuring a customizable wearable design with 4 electrodes and a specialized complex-valued impedance sensing board
- two datasets with 15 participants featuring electrical impedance signals of 7 micro-gesture events and continuous pinch forces in Newtons

- machine learning algorithms for micro-gesture recognition and continuous pinch force estimation, as well as few-shot learning models for generalizability and applicability
- evaluation of our approach on micro-gesture recognition and pinch forces estimation using Leave-One-Subject-Out (LOSO) cross validation
- three applications for enhancing user experiences in augmented and interactive technology, extended reality (XR), and assistive technologies.

## 2 Related Work

Our work intersects the following three major domains: 1) wearable-based gesture recognition systems, 2) on-body force sensing systems, and 3) electrical impedance based user sensing approaches.

### 2.1 Wearable Micro-gesture Recognition

Hand micro-gesture sensing is crucial for ergonomic, intuitive, and subtle interaction with computing systems around us [3, 23, 53]. Predominant approaches for wearable micro-gesture recognition have relied on vision-based systems, utilizing optical sensors [4, 48, 56] and IR cameras [12] and sensor fusion of acoustics and optics [54]. However, these camera-based methods face limitations in terms of privacy, power consumption, resilience to lighting conditions, and visual occlusion artifacts. In contrast, non-optical methods, although less extensively explored for hand sensing, have emerged as a promising lightweight alternative. Approaches along these lines have instrumented the whole hand [33, 41] with gloves or sensors on each finger. Ring-based [28, 44] sensing interfaces have been explored as a more practical form factor but are limited in their sensing fidelity to the particular finger of instrumentation.

In contrast, wrist-worn devices serve as a more ubiquitous, portable and accessible interactive platform with minimal obtrusiveness, allowing to sense the whole hand from a single point of instrumentation. While works along these lines have looked in acoustic [19], Electromyography (EMG) [31], optical [10, 16] and RF [21] for coarse hand pose sensing, they lack the fidelity for fine-grained micro-gesture recognition. In this regard, inertial sensing methods have seen success on consumer form factors. Apple Watch and Galaxy Watch have released assistive features detecting double pinch and hand grasp models based on IMU and PPG [1, 38]. Viband [26] utilized high sample rate accelerometers in commodity smartwatches to observe pinch down, flick, and snaps. However, these inertial-based methods lack the fidelity to capture more subtle micro-gesture traits that do not create a large motion signature, such as thumb swipe direction, pinch finger release detection, pinch finger recognition, or pinch pressure.

Closest to our work are EMG-based micro-gesture recognition [25, 51] works that sense the electrical potential of muscle contractions with high sensitivity. Unfortunately, these systems require between 16 to 64 electrodes placed on the forearm, where signal-generating muscle fibers are most plentiful, and therefore do not align with potential integration into a smartwatch form factor. Instead, for our system, we turn to electrical impedance measurements. As an active sensing method, electrical impedance does not require dense muscle fibers for a sufficient signal, allowing our system to sit at

the wrist, using only 2 pairs of electrodes total, and ensuring a light-weight minimal design with potential to integrate with commercial smartwatches (Section 8.4).

### 2.2 On-body Force Sensing

In addition to microgestures, our system also senses continuous pinch pressure. Here we discuss methods of on-body force sensing technologies, which aim to measure contact forces exerted by or onto the human body, enabling continuous and fine-grain interaction. Approaches in this space range from mechanical [40] and material-based sensing [30] to physiological signal-driven inference methods [8]. One common category includes resistive and capacitive sensors that directly capture surface deformations. For example, force-sensitive resistors (FSRs) are widely used in commercial applications for surface contact pressure measurement [37], while capacitive-based sensors have been implemented in devices like Apple's 3D Touch. Recent work [57] has also explored force estimation using capacitive image sequences to detect subtle force variations through skin contact. Hybrid approaches such as iSkin [52] integrate both capacitive and resistive sensing into soft, deformable electronics for wearable pressure input. However, these approaches require direct contact between the sensor and the point of interaction (e.g., placing sensors at the fingertip for pinch force detection), which is not ideal for wrist-worn or distal sensing applications. Such placement often interferes with natural hand movement, limits wearability, and may not generalize well to everyday usage where minimal instrumentation is preferred.

More precise force readings have also been enabled via vision-based methods. GelSight [58] and other optical tactile systems measure surface normal forces via internal gel deformation captured by embedded cameras. Similar techniques have been adapted for head-mounted cameras to infer pinch forces [32]. However, vision-based methods often face challenges in mobile scenarios due to power, occlusion, and privacy concerns, making them less suitable for mobile or continuous use. Mechanical designs have also been used to infer force, where deformation of physical components (e.g., springs) is used to estimate pressure. The Pinch Sensor [50] and Squeezzy-Feely [40] demonstrate mechanical pinch and grip sensing through deformation-based feedback. While robust, such solutions often trade off bulk and form factor for measurement fidelity. Physiological signal-based approaches using physiological data such as EMG have also been explored for pinch force estimation. For example, Choi et al. [8] and TouchSense [2] use EMG signals to infer contact force but often require high-density sensor arrays across forearm to upper palm and rigid body contact, limiting their applicability in wrist-worn form factors and subtle finger movements.

Unlike these prior works, which either require rigid contact, extensive instrumentation, or do not target subtle wrist-based interactions, EI-Lite estimates continuous pinch force from only the wrist area using electrical impedance signals alone. To our knowledge, EI-Lite is the first wearable to demonstrate real-time, contact-free pinch force estimation via bio-impedance sensing. This enables pressure-aware interactions with minimal hardware and obtrusiveness, making it highly suitable for mobile and assistive applications.

### 2.3 Electrical Impedance Based User Sensing

Since first being proposed in 1978 [14], Electrical impedance sensing has served as a non-invasive medical imaging method to examine breast cancer [65], brain function [36], and cardiac, lung, and pulmonary health [15]. By measuring the impedance between electrodes distributed around an object’s perimeter in a round-robin fashion, an impedance map of the cross-sectional area can be back-projected. In recent years, low-cost impedance front-ends have allowed for more accessible electrical impedance sensing device prototyping. Electrick [60] uses several electrodes placed around a conductively-coated object for rich touch sensing. Zhu et al. [64] introduced an open-source EIT toolkit for designing and fabricating EIT devices for health and motion sensing, with later applications to muscular rehabilitation [63] and liquid identification [62]. The non-invasive and non-line-of-sight qualities of electrical impedance sensing have also made it appeal to human motion sensing.

Electrical impedance sensing has also been leveraged for various hand sensing tasks. At the index finger, ElectroRing [20] uses an injected signal to robustly determine pinch closure between the thumb and index finger. Z-Ring [47] uses a wideband RF sweep from an off-the-shelf VNA at the finger base to recognize thumb-to-index finger microgestures, held object recognition, and user identification. Z-Pose extends this technique to determine hand pose [49]. Unlike these finger-worn systems, we seek to enable wrist-based micro-gesture and pinch force sensing. In addition, EtherPose [21] uses two cloverleaf antennae at the wrist for hand pose, but due to its over-the-air impedance measurement method, these antennae are each approximately 2 cm in diameter to operate within a frequency range influenced by hand pose. Our system instead leverages more conventional galvanically injected impedance measurements, which can be achieved with low-profile dry electrodes.

Most similar to our work are the systems derived from electrical impedance tomography that sense the hand from the wrist. Tomo [59] utilized between eight electrodes around the wrist or forearm to determine static hand poses with 86.5% within-user accuracy and 59.6% cross-session accuracy for a gesture set with pinches between the thumb and each finger and no null class. Further work [61] increased accuracy by adding additional electrodes at the forearm, i.e. up to 32 electrodes, yielding up to 94% cross-session accuracy. Most recently, EIT-Pose [24] used sensing hardware improvements and eight electrodes around the forearm to determine hand poses.

As compared to these systems, EI-Lite targets a more subtle micro-gesture set for device control in a more practical package – one that is more amenable to smartwatch integration. In addition, previous approaches only explored the real part of the impedance signals. For EI-lite, a customized impedance sensing board is implemented for accurate imaginary part impedance sensing as well, and operates at a much higher system sampling rate (100Hz vs. EIT-Pose / Tomo’s 10Hz), which are essential for the subtle and imperceptible finger movements during micro-gesture and pinch pressing activities. As a result, EI-Lite can achieve more than hand gesture recognitions, but also continuous pinch force estimation, which are not possible with prior EIT works, while keeping a minimized system design.

## 3 EI-Lite System Overview

The EI-Lite system contains two parts: (1) a wearable adjustable sensing wrist band around the distal radioulnar joint with 4 electrodes (minimum number of electrodes required for 4-terminal measurement), and (2) a custom-designed impedance sensing board. The individually adjustable 4 electrodes are placed on top and bottom of the wrist in a 2-by-2 setup. This configuration can be integrated into existing smart watch and band designs (e.g., Google Pixel Watch) with minimum effort. For example, this can be achieved by placing two electrodes on the back of the watch dial and two on the band buckle. The sensing location around the wrist and the specific electrode locations are driven by the electrode location and ablation study detailed in the Section 4. The custom impedance sensing board is designed based on the MuscleRehab [63] schematics, an EIT sensing board specialized for muscle engagement monitoring. Compare to the MuscleRehab board, our board features several major design improvements optimized for high frequency injecting channel switching, which enables high sampling rate (up to 100 Hz) required for micro-gesture detection and continuous pinch force estimation, reliable real and imaginary parts impedance sensing, and a much more compact design for wearable applications.

### 3.1 Wearable Sensing Wrist Band

The electrical impedance sensing wrist band consists of a wrist-worn ribbon and 4 individual sensing units (Figure 2a&b). The wrist-worn ribbon (0.6cm×27cm×0.05cm) is 3D printed with TPU and lined up with slots (0.2cm×0.3cm) every 0.3cm. One end of the ribbon has two extruded buttons that can be inserted into the slots to create an adjustable wristband for wrist circumferences ranging from 10 to 22 cm. The 4 individual sensing units each consists of a case, a brass ball, and a ring terminal. The case (1.7cm×2.2cm×0.7cm) is 3D printed with PLA and consists of two parts that can be tightly locked with a snap-fit joint after the components are placed within. The case has two slots on both sides for the wrist-worn ribbon to thread through, with just enough flexibility for adjustable positioning of the unit while having enough friction to keep it in place. The brass ball (3/8" diameter) fits tightly inside the case, mechanically connected to the ring terminal, with one third of its height exposed at the bottom to be in contact with the skin, allowing for a point-contact at desired location for each user to optimize accuracy. Finally, the ring terminals are connected to multi-thread wires via the crimping tool to transmit the AC signal from and the resulting voltage response to the sensing board. Overall, the wearable form factor is designed to be lightweight, small, and flexible.

### 3.2 Impedance Sensing Board

For better integration with the wearable form factor, we implemented a customized slim electrical impedance sensing board (2.5 cm × 7 cm), which is built around a Teensy 4.0 microcontroller, and responsible for injecting the AC signal and measuring the resulting voltage response across all pair combinations of the 4 electrodes (in total 6 measurements). The impedance sensing board consists of two main parts: a current drive circuit for injecting the AC signal, and a voltage response measurement circuit for measuring the voltage output (i.e., signal amplitude and phase) from the current drive.

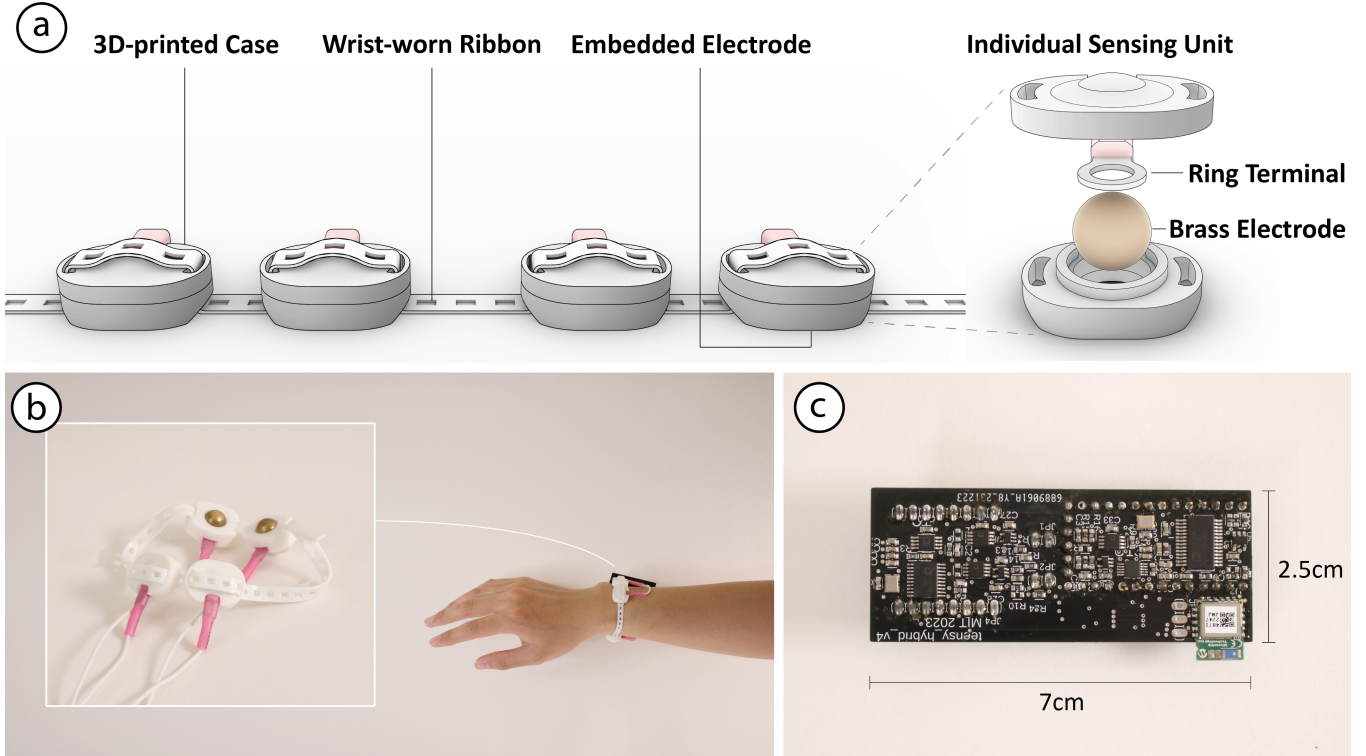


**Figure 2: EI-Lite system overview.** (a) The design layout of our wearable electrical impedance sensing wrist band, with 4 individually adjustable electrodes. (b) The electrodes are placed on top and bottom of the wrist’s distal radioulnar joint in a 2-by-2 setup. (c) The coupled readout circuit board to serialize electrical impedance readings.

The current injecting circuit is composed of a signal generator, an adjustable instrumentation amplifier, and a voltage-controlled current source (VCCS). Specifically, the signal generator (AD5930) serves as a voltage source and generates a small, constant-amplitude, differential sine waveform at 50kHz frequencies.

Compared to the original MuscleRehab and EIT-kit board design, we have implemented several major updates over both current drive and voltage response measurement circuits, so that we are able to reliably sense imaginary impedance signal at high system sampling rate (100 Hz). First of all, the run-time-settable signal strength is now controlled in a linear fashion by varying a reference voltage used by the AD5930 function generator via a DAC (Digital-to-Analog Converter). Using a 12-bit AD5620 DAC, the improved design approximately gives 11 bits or (2358 values to be exact) of drive strength, settable with an adjustment time of roughly 0.5 ms. In both the micro-gesture recognition and pinch force estimation, we set the signal amplitude and frequency to be 1mA at 50kHz.

The second major improvement addresses the drift issue inherent to conventional Howland current sources, which ideally maintain a constant current only within a narrow voltage range. Rapid electrode array switching (e.g., during high sampling rate) and human tissue interactions (where there can be non-zero voltage offsets from electrodes) exacerbate voltage drift, causing the circuit to hit power rails, temporarily losing current-source behavior. To mitigate this, we redesigned the circuit using instrumentation amplifiers for its Howland Current Source networks, with internal laser-trimmed

resistors and buffered feedback (two unity-gain op amps sown) to achieve better balanced current source in a Mirrored Howland Circuit and minimize drift. Given the high-output impedance of the mirrored Howland configuration, we introduced high-value bias resistors connecting each drive electrode to  $V_{cc}/2$ . These resistors establish a stable mid-supply reference, preventing voltage accumulation and rail saturation, thereby preserving ideal current-source performance during continuous electrode switching.

In addition, on the sensing software side, the system injects an integer number (exactly 7 cycles) of stimulating cycles per measurement and compares injection signals against the waveform generator flags in real time. This ensures minimal stray voltage accumulation during rapid electrode switching, preserving accurate imaginary impedance measurements. The voltage response circuit captures differential signals from four electrodes via dual multiplexers (ADG731), feeding two unit-gain input buffers (ADA4841) with 350 Hz high-pass filters. The buffered signals pass through an adjustable-gain instrumentation amplifier (AD8220, modulated by AD5260), scaled from 3.3 V to 1 V, and filtered again (1 kHz–1 MHz band-pass). Finally, a 10-bit ADC (AD9200) digitizes the filtered output at 20 MHz.

#### 4 Electrode Location & Ablation Study

To overcome the challenges of impedance signal variances due to complex anatomical structures, we conduct a user study with 13 participants to evaluate which area around the wrist is the most

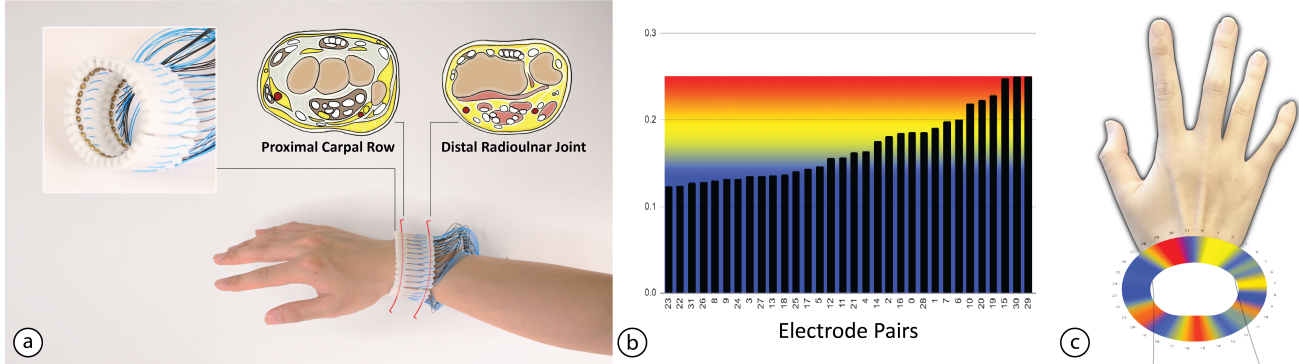


**Figure 3: Electrode Location & Ablation Study.** (a) The user study was performed by capturing electrical impedance signals from 2 by 32 electrodes around both proximal carpal row (L1) and distal radioulnar joint (L2) area. (b) The electrical pairs' signal effectiveness ranking in red-to-blue color spectrum. (c) The signal effectiveness heat map around the wrist area in red-to-blue color spectrum.

optimized location for sensor placement for subtle finger movements across users. To achieve this, we capture electrical impedance signals from various locations around the wrist, identifying the positions that consistently produce the strongest and most reliable signals across users. In this section, we outline the design of the study and the key findings that inform the most effective electrode placements for EI-Lite system design.

#### 4.1 Study Setup

We recruited 13 participants (8 males and 5 females), and all participants used their right hand for the study for consistency. We designed a flexible and adaptive sensing wristband that fits users with wrist sizes from 14cm to 20cm. The wristband is integrated with 64 individual electrode units in a  $32 \times 2$  layout, covering both proximal carpal row (L1) and distal radioulnar joint (L2) area evenly, as shown in Figure 3a. This adaptive design ensures that the relative positioning of each electrode remains consistent on the wrist across different users. During each data collection session, participants are instructed to move one finger at a time, then two fingers together, and so on up to five fingers simultaneously, covering all possible finger combinations (in total 31 finger combinations). This is followed by a 30-second period of free movement. Each user performed 3 data collection sessions for each of the wrist locations (L1 and L2), with each session lasting ca. 1.5 min.

The data collection is conducted inside of a motion tracking camera booth with 18 synchronized cameras recording the finger positions and hand poses at 30 frame-per-second. The impedance sensing board is programmed to sample at 3.3 Hz. The finger and hand positions ground truth are generated via triangulation on the 21-keypoint MediaPipe results over each camera's frame. In total, 14484 frames of data were collected (7494 for L1 and 6990 for L2), each frame contains 1024 ( $32 \times 32$  impedance measurements).

#### 4.2 Results

We assess the quality of electrical impedance sensing signals from L1 and L2 by evaluating their performance in gesture recognition.

This task is selected because it closely resembles our task of micro-gesture recognition, involving similar movements of tendons and muscles around the wrist. More specifically, we built two ML models for 21-keypoint location prediction for the proximal carpal row (L1) and distal radioulnar joint (L2) areas data. The two models use the same ExtraTreesRegressor from SciPy, similar to the model architecture used in the previous works [24].

The results show the mean per joint positional error at L1 and L2 to be 25.35 mm and 13.0 9mm respectively, indicating that the distal radioulnar joint (L2) area is a more accurate and generalizable location for micro-gesture recognition via electrical impedance sensing across users. This result came as a surprise, as the proximal carpal row (L1) area should in theory perform better because it is more anatomically aligned with individual finger movements, and it was performing better during pilot study with 2 users and for the general dataset if model is trained & tested within single user's data. However, the distal radioulnar joint area turned out performing better across users. We hypothesize that this might be due to the proximal carpal row area is: (1) much more complex anatomically therefore more variance between different human subjects, and (2) too close to the hand movement which likely leads to a lot of skin friction noises introduced during micro-gesture movements that might result in different wrist-to-hand movement / orientation, whereas the distal radioulnar joint is considerably more stable during the hand movements. More thoroughly studies are needed to further verify our hypotheses.

In addition, to minimize the number of electrodes for our design for device wearability and higher sensing FPS, we conducted an electrode ablation evaluation based on which electrode pairs around the targeting wrist sensing area contain most impedance changing information during the micro-gesture movements. Each electrode pair refers to the adjacent electrodes in L1 or L2 area, and was measured separately. We then calculated the relative impedance reading changes (i.e. signal standard deviations) measured at each pair location (in total 32) for all users when performing each gesture movement, and use that as an indicator for how "strong" the signals are at that pair location across users. We ranked them from

high to low, the higher the more impedance changing information that electrode pair channel is consist of. More detailed results with individual rankings and the overall signal heat map around wrist area are shown in the Figure 3b&c. The results indicate that approximately the top and bottom areas of the wrist contain the most impedance changing information during the micro-gesture movements. Therefore when designing the EI-Lite wearable sensing wrist band, we decided to place the 4 electrodes on top and bottom of the wrist (distal radioulnar joint) area in a 2-by-2 setup to maximize the signal effectiveness.

## 5 Micro-Gesture Recognition

In this section, we present the data collection protocol, data pre-processing methods, model architecture, and results of micro-gesture recognition.

### 5.1 Data Collection

To accurately collect multi-channel electrical impedance data during each of the micro-gesture movement, we implement a synchronized data collection setup with a commercial Force-Sensitive Resistor (FSR) directly connected to our EI-Lite device. More specifically, we fix the FSR (Interlink Electronics FSR 400 Short, 5mm diameter Circle [18]) to the tip of the thumb, and use the synchronized force reading as an indicator of the start and end of each micro-gesture event. We adapted this FSR sensor on finger approach for contact & force detection from previous work [32]. We chose a FSR size much smaller than typical thumb area to ensure the thumb can physically contact the other hand parts during each gesture without being covered, so that the impedance measured is as close to the condition where there is no FSR present as possible. In addition, we adapt the FSR placement based on each user's habit, i.e. we ask them to perform all the micro-gestures before data collection and place the FSR at the center of their natural contact area on the thumb to achieve more accurate and synchronized reading.

In order to capture the subtle and swift changes during micro-gestures, our device is set to record at 100 frame-per-second, which is within the typical sampling rate range for IMU-based approaches [55] and align with our data collection pilot study experience. Each captured frame contains 6 individual measurements with 12 values, with both real and imaginary parts for each measurement. During each data collection session, the participant follows instructions displayed on a laptop screen and performs each of the six micro-gestures repeatedly for one minute at their own comfortable pace, followed by a 30-second idle state. Each participant completes 3 data collection sessions. During data collection users were not required to use any specific arm / hand pose for their sessions, yet they were asked to sit still during each session, but free to change between sessions. To ensure a diverse dataset and prevent overfitting, the device is removed between sessions, and participants engage in unrelated tasks during these breaks.

### 5.2 Dataset Pre-processing

Since the dataset was recorded continuously, there are large sections of idle state between sequences of valid micro-gesture events. To maintain a balanced dataset for learning and minimize the impact of unrelated signals, we pre-process the data to extract valid windows

for each of the seven micro-gesture events (six gestures and idle state), which serve as individual input data points for our model, as shown in Figure 4. Valid signal sequences are first identified based on synchronized FSR sensor readings, indicating where each micro-gesture occurs. We then apply a sliding window approach to extract 60-sample windows (equivalent to 600 ms in real time) from these sequences, following specific criteria. Detailed pre-processing criteria for each micro-gesture category are provided below. Note that FSR forces sensor's reading below 1 N are considered as zero.

*Pinch Start:* For index and middle pinch start signals, valid signal sequences are identified by allowing between 40 and 10 consecutive zero samples before the FSR signal's rising edge. Additionally, a minimum of 5 consecutive non-zero samples apart from the FSR signal's falling edge is required. Then valid data windows are extracted through window-sliding with a stride of 8 samples.

*Pinch Release:* For index and middle pinch release signals, valid signal sequences start with the FSR signal's peak and end 15 samples before the next rising edge. Valid data windows are extracted using a sliding window approach with a stride of 8 samples. Each window must contain at least 5 non-zero samples (i.e. the pinch release event lasted for less than 0.05 second are discarded).

*Swipe:* For the swipe left and swipe right signals, valid signal sequences are selected with up to 20 zero samples and at least 4 consecutive zero samples before the FSR signal's rising edge. Valid data windows are extracted through window-sliding with a stride of 8 samples.

*Idle State:* For the idle states data windows, we extract directly from idle sections at 4 samples per stride (since at idle state, the FSR readings are all at 0). Comparable numbers of data points are extracted for a balanced dataset.

In total, 35680 valid data windows for 7 micro-gesture events were collected across 15 users, including 6015 windows for idle state, and up to 5553 for each single micro-gesture.

### 5.3 Model

Our model takes in a 60-frames time series of 12-channel electrical impedance data sampled at 100hz, resulting in an input shape of (60, 12). This input time series spans 0.6 second in total while incorporating a 0.3-second look-ahead time. The output of our model is a (1, 7)-shaped vector probabilities of the seven micro-gesture events. We pass each input window through two Conv1D layers with 32 and 64 filters, respectively, both using ReLU activation and followed by batch normalization and max-pooling layers. After feature extraction, the data is flattened and passed through a dense layer with 64 units, concluding with a softmax output layer for classification. The model is trained by minimizing the categorical cross-entropy loss using the Adam optimizer at the learning rate of 0.001. Our model consists of 20,631 parameters, occupying 81 KB of memory, making it suitable for on-device execution. Using one V100 GPU, we are able to train the model in under an hour.

Additionally, to improve the generalization of our model across users, we adopt a few-shot learning approach [42], as demonstrated in Figure 5a. We fine-tune the pre-trained classifier using up to 40 windows of data from previously unseen participants. This fine-tuning process refine the model weights through full network back-propagation and takes less than a minute. We experimented with

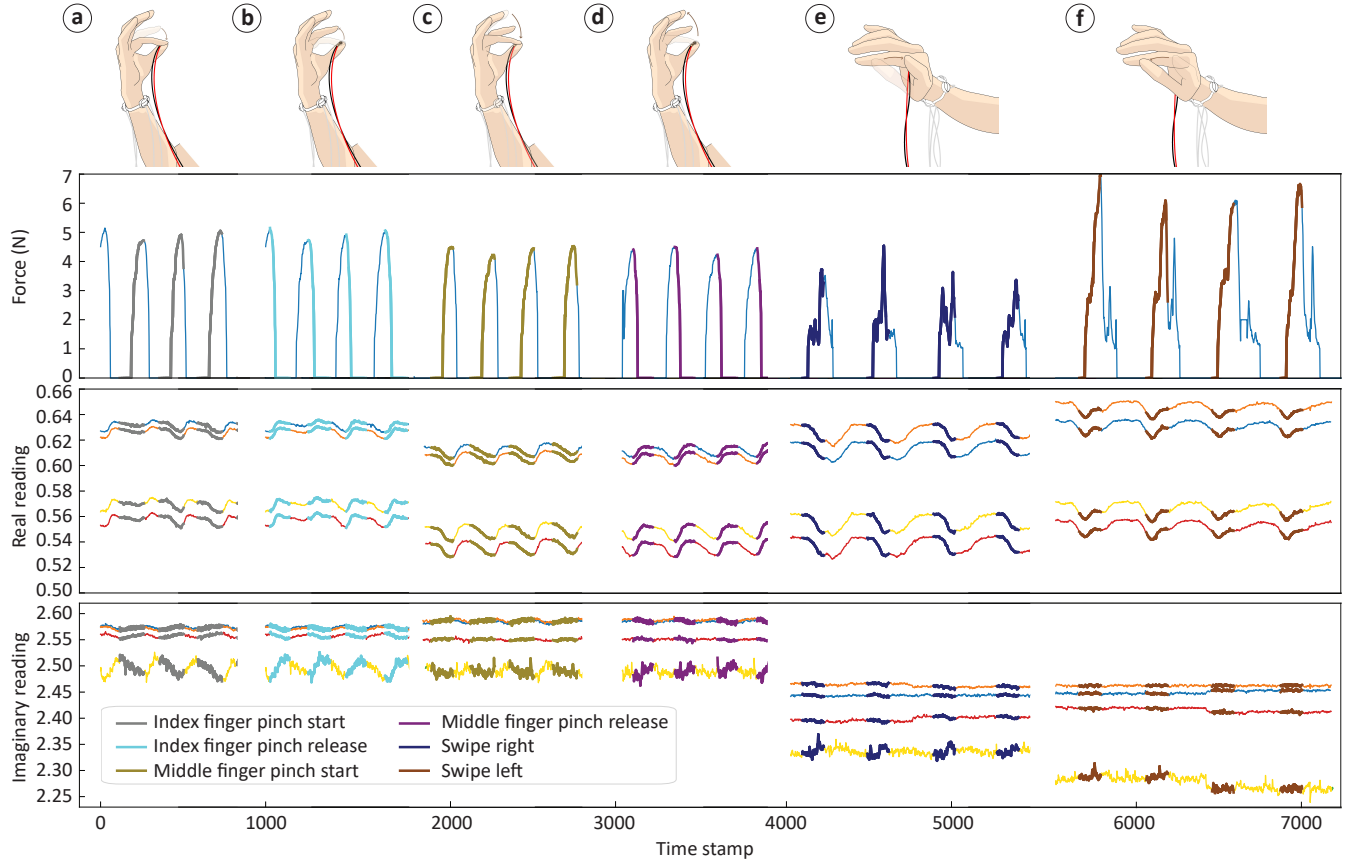


**Figure 4: Synchronized force-sensitive resistor readings and electrical impedance signals for (a) index finger pinch start, (b) index finger pinch release, (c) middle finger pinch start, (d) middle finger pinch release, (e) swipe right, and (f) swipe left.**

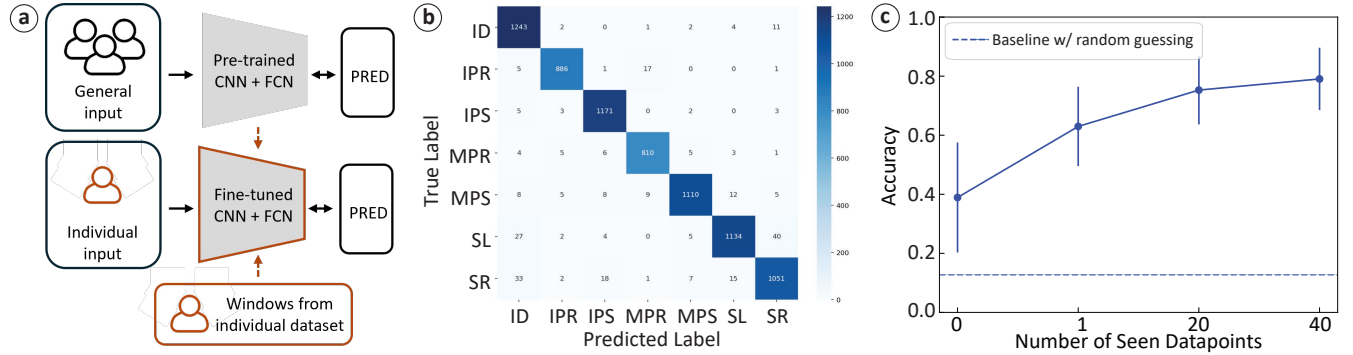


**Figure 5: Micro-gesture recognition.** (a) We leverage a few-shot learning approach to improve the generalization of our model on unseen users. (b) Overall, our model achieves a classification accuracy of 96.33% on seen users and (c) up to 80.6% on unseen users with limited user examples.

different fine-tuning strategies ranging from one window size to a full-session of unseen data, to evaluate the influence of calibration data length on model performance and generalization. Our model evaluation follows a standard Leave-One-Subject-Out (LOSO) cross-validation procedure.

## 5.4 Results

Using 80% of the full dataset (across all users) for training and validation, and the rest for testing, we achieve a classification accuracy of 96.33%, as demonstrated in Figure 5b (and ca. 16% higher than

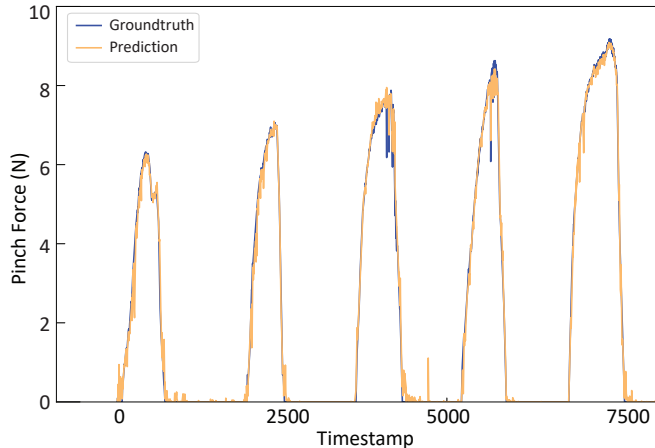


**Figure 6: Pinch force estimation result. The predicted pinch force aligns with the ground truth captured by the force-sensitive resistor.**

using the electrical impedance real part signal only). We then assess the model’s generalizability across unseen users. Given the unique characteristics of each user’s hand structure, the electrical impedance signals display highly distinctive features. This variance leads to a notable decrease in classification accuracy to 37.7% when applied to unseen users. Using a few-shot learning technique, we improve the performance of our model on unseen users by incrementally increasing the number of observed windows from 1 to 40, where each window consists of 60 frames and is equivalent to 0.6 seconds in real time. The few-shot learning approach leads to a significant boost in classification accuracy, reaching 80.6% with 40 observed windows or just 24 seconds of data (Figure 5c). It demonstrates the effectiveness of few-shot learning in adapting the model to diverse hand structures and improving its performance on new, unseen data.

## 6 Continuous Pinch Force Estimation

In this section, we present the data collection protocol, data pre-processing methods, model, and results of continuous pinch force estimation.

### 6.1 Data Collection

Similarly to the data collection setup in the Micro-gesture event recording, we attach an FSR to the upper area of the thumb and use the synchronized FSR force readings to capture real-time pinch forces for supervision. During each data collection session, the participants are instructed to press on the thumb with the attached FSR sensor using their index finger, gradually increasing the pinch forces until they reach the maximum force they would consider as a "hard pinch". They then gradually decrease the pinch force until the index finger is no longer in contact with the thumb. The participants are instructed to perform this movement for 10 times, with a total duration of ca. 1 min to 1.5 min. Again, each participant is asked to record 3 such pinch force data collection sessions, in between which the devices are taken off from the participants.

### 6.2 Dataset Pre-processing

The pre-processing of pinch forces dataset is straightforward, as the impedance and FSR force reading are sampled at the same 100Hz with a 1-to-1 correspondence with our electrical impedance signals. According to the FSR datasheet [18], we first filtered any force readings less than 0.3 N as 0 N to eliminate noises. We then apply a sliding window approach to extract 10-sample windows (equivalent to 100 ms in real time) from each data collection session, with corresponding ground truth as the mean of the 10-sample window force readings in Newton. In total, 351239 samples are collected for the dataset across 15 participants.

### 6.3 Model

We estimate pinch forces in a continuous manner through a RandomForestRegressor, with 200 estimators. This model takes in a time series of electrical impedance data, with a shape of (10, 12) and outputs a pinch force prediction in Newtons. The model is tested in two scenarios: (1) a standard train-validation-test split with 70% training data, 10% validation data and 20% test data, and (2) Leave-One-Subject-Out (LOSO) cross-validation. Performance is assessed using mean squared error(MSE) and  $R^2$  score.

To enhance generalizability, we also implement a CNN-based neural network with three convolutional layers (32, 64, and 128 filters), each with a kernel size of 3 and ReLU activation. A Global-AveragePooling1D layer reduces dimensionality, followed by fully connected layers (64, 32, 16 units) with ReLU activation. A final sigmoid-activated neuron outputs a pinch force percentage relative to the maximum detected for each user. The model is trained using the Adam optimizer (learning rate = 0.001) and MSE loss. Evaluation follows the same LOSO protocol, with MSE and mean absolute error (MAE) as key metrics. This model has a total of 42,977 parameters, occupying 167.88 KB memory, suitable for real-time on-device inferences. Training on a V100 GPU is completed in under an hour.

We experiment with input sequence window sizes of 10, 20, and 40 frames to assess the impact of sequence length on feature extraction and model accuracy. Each window size was tested to evaluate the trade-off between prediction latency and the ability to capture temporal dependencies for more accurate prediction. Furthermore, we experimented with varying amounts of calibration data, ranging from 0 (no calibration) to 40 seconds of calibration data from unseen participants, to evaluate its influence on model performance and generalization. This test help assess the trade-off between the quantity of calibration data (or length of calibration time) and the model’s accuracy and generalization capabilities.

### 6.4 Results

Using 80% of the full dataset (across all users) for training and validation, and the rest for testing, we are able to estimate the pinch force with a mean-squared-error (MSE) of 0.3071 or mean-force-variance (RMSE) of 0.55 N. As demonstrated in Figure 6, our model predicts the pinch forces in a continuous manner, aligning with the groundtruth captured by the FSR sensor. However, our model fails to generalize to unseen users, as evident in Figure 7a top-left panel. This can be explained by our observation of the significant variation in individual pinch force ranges, which span from 5.41 N to 12.67 N.

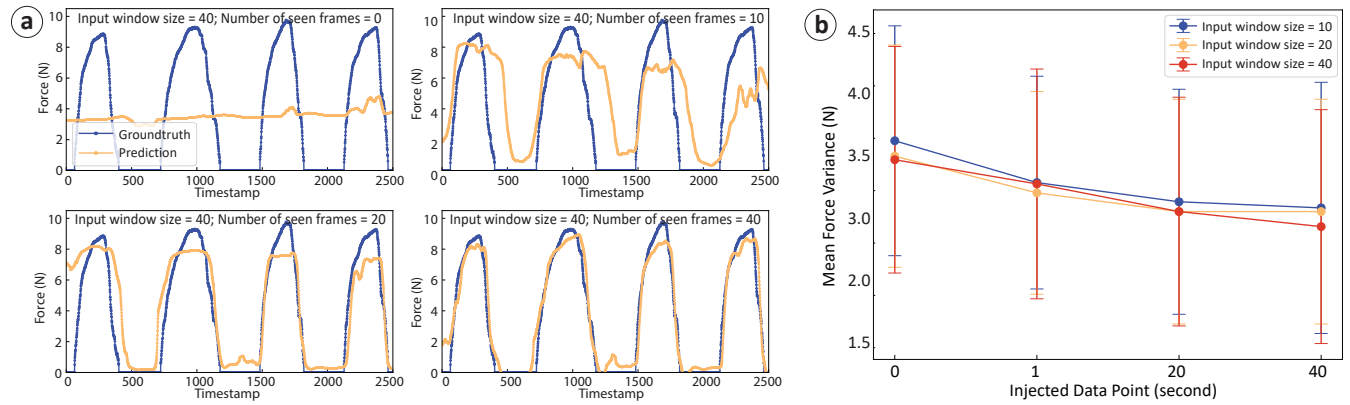


**Figure 7: Generalization of pinch force regressor on unseen users. The performance of our model improves with (a) the addition of more injected frames for few-shot learning and (b) an increase in input window size.**

While the electrical impedance signals effectively capture the patterns and trends of pinch forces for each user, they can not estimate the force range accurately without prior exposure to specific user data. To this end, we enhance the model’s generalization by refining the pre-trained model with up to 40 windows from previously unseen users. As demonstrated in Figure 7, the predicted pinch forces increasingly align with the ground truth, with a decreasing mean force variance as the number of injected windows increases. Additionally, the model’s performance improves with larger input window sizes (Figure 7b). This is expected, as larger input windows provide more information, though they also introduce a trade-off for real-time estimation, as larger windows result in longer delays. Overall, we are able to retrieve reliable pinch force predictions for unseen users via the few-shot learning approach.

## 7 Applications

EI-Lite’s compact, wearable design and ability to accurately recognize micro-gestures and estimate pinch force make it well-suited for enhancing user experiences in extended reality (XR), augmented and interactive technology, and assistive technologies.

### 7.1 Extended Reality (XR)

In this paper, we use the term XR to encompass Augmented Reality (AR), Virtual Reality (VR), and Mixed Reality technologies. Hand gestures stand at the center of new XR interaction paradigms, as seen in commercial products like Vision Pro and Oculus hand tracking systems, due to the freedom of movement they provide users. While current XR devices predominantly employ vision-based methods for hand gesture recognition, this significantly constrains interaction by requiring hands to remain within the camera’s field of view of the HMD. In addition, even within the camera view point, there is no robust method for fine-grained finger pressing and pinching input.

Our electrical impedance-based interface addresses these limitations by enabling micro-gesture input regardless of hand position relative to the headset’s cameras, substantially increasing hand freedom compared to existing methods. We implemented two XR applications to demonstrate this capability. Figure 8 demonstrates

intuitive micro-gesture control in a 3D RPG game, where players can open or close inventory window (index pinch and release), switch weapons in floating windows (left or right swipe), and view weapon’s pop-up descriptions (middle pinch and release). This implementation would create a more intuitive gaming experience by eliminating the need for traditional controller buttons or complex menu navigation. Players can maintain immersion in the game world while performing common actions through natural hand movements, even when their hands are not directly visible to the headset’s cameras. The system’s ability to distinguish between different finger pinches and directional swipes provides sufficient input variety for complex game mechanics without requiring visual line-of-sight to the user’s hands, offering considerable advantages over conventional vision-based hand tracking systems in gaming contexts. In addition, Figure 9 shows how pinch force detected through EI-Lite can be applied to virtual objects, enabling not just kinematic interactions that simulate appearance of motion, but also kinetic interactions that replicate physical forces—the interacting fruit object deforms according to applied pinching forces, and when the force exceeds 6N, the fruit object bursts.

### 7.2 Interaction Control for Daily Activities

Micro-gesture recognition using EI-Lite enables seamless interaction with everyday devices. This technology can be applied to smart home environments, allowing users to control household appliances such as lights, thermostats, entertainment systems, and smart displays through intuitive gestures. For instance, a simple pinch gesture could turn lights on or off, while swipe gestures might adjust temperature settings or audio volume. The electrical impedance sensing technology provides significant advantages over camera-based systems by functioning regardless of lighting conditions or direct line-of-sight to the controlled device. Additionally, it offers a natural interface for PC operations such as presentation control, document navigation, and media playback without requiring physical contact with traditional input devices.

Figure 10 showcases a presentation control application demonstrating this capability. Users can start slideshows with an index finger pinch and release, end presentations with a middle finger pinch

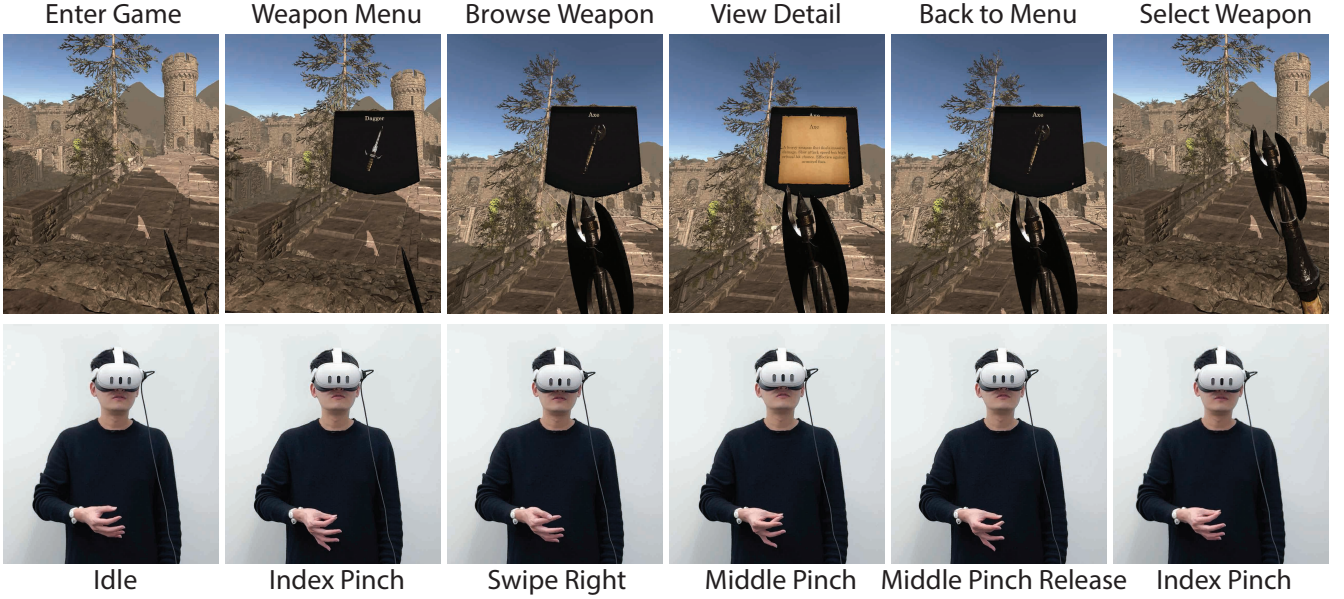


**Figure 8: EI-Lite for VR gaming.** A user open the weapon menu, swipe between floating menus, view pop-up details window, and select new weapon by performing different micro-gestures wearing EI-Lite.

and release, and navigate between slides using left/right swipes. These micro-gestures, detected through electrical impedance, offer discreet interaction particularly valuable in public speaking scenarios where maintaining audience engagement is crucial. This implementation would create a more intuitive presentation experience by eliminating dependence on remote controls or keyboard shortcuts, allowing presenters to move freely throughout the presentation space while maintaining seamless control of digital content.

### 7.3 Assistive Technology

Our research also offers significant potential for accessibility applications. The academic community has developed numerous exoskeletal systems using muscle activity for rehabilitation and assistive purposes [6, 9]. As our technology evolves to predict increasingly diverse and small hand movements, it could make revolutionary contributions to prosthetic exoskeleton development and other assistive technologies.

This technology particularly shines in assistive control applications. For example, individuals who suffer from extremity amputation or with limited hand function could still perform some interactions that typically require two hands. Figure 11 demonstrates this capability through our application that enables smartwatch control via one-handed micro-gesture recognition. Users with arm/hand injuries or those who have experienced unilateral extremity amputation can still control their smart watch, such as music playback on Spotify using index finger pinch gestures to start/pause music, and swipe left or right to navigate to next or previous songs. This approach could play a crucial role in creating more inclusive digital experiences, significantly enhancing accessibility for individuals with physical disabilities and promoting more equitable participation in both virtual and physical environments.

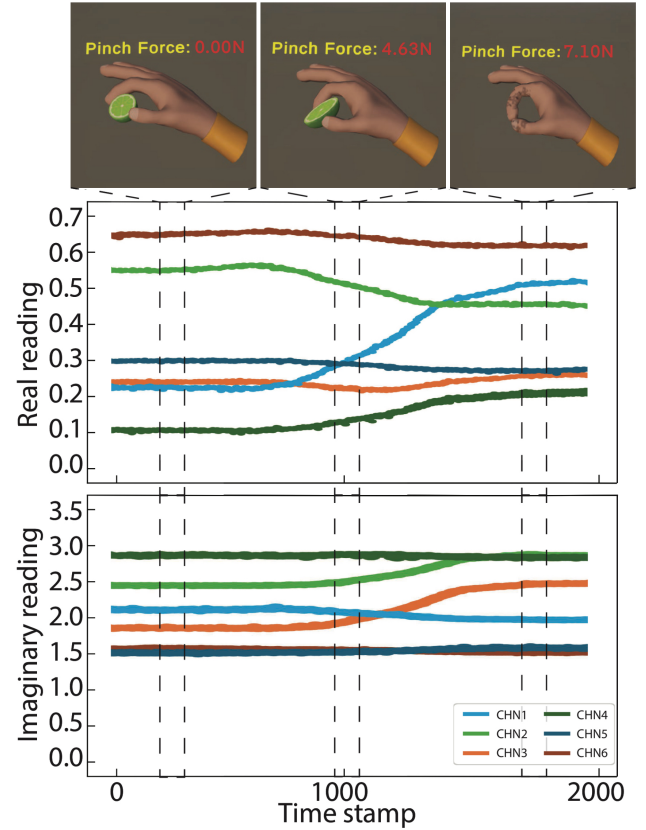


**Figure 9: EI-Lite for force estimation in XR.** EI-Lite estimates the pinch forces through electrical impedance readings and projects it to an XR scenario.

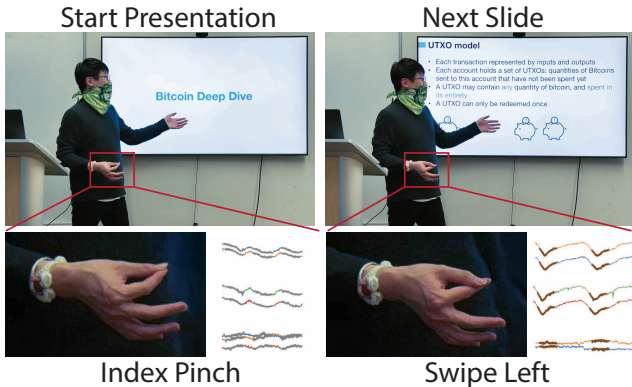


**Figure 10: EI-Lite for presentation control.** A user pinches with different fingers to start & end the presentation, and swipes left / right to next / previous slides.



**Figure 11: EI-Lite for accessible smartwatch control.** A user with limited hand functions performs one-handed micro-gestures to control a smartwatch.

## 8 Discussion and Future Work

In this section, we discuss some limitations and future work directions of our EI-Lite system, including the electrode design form factor, limitations of our current data collection methods, potential future improvements over the ML model generalizability, and our insights on how the EI-Lite approach can be integrated with commercial smartwatch designs.

### 8.1 Electrode Form Factor

Current designs rely on rigid electrodes, which are not the most practical and comfortable option for wearable interactive devices. In future iterations, these electrodes could be optimized for greater flexibility and wearability. For instance, integrating the electrodes directly into a wristband using conductive fabrics [62] could provide a seamless solution, eliminating the need for bulky 3D-printed electrode casings. This approach would not only enhance user comfort but also allow for more natural and unobtrusive wear, improving long-term usability in everyday environments. Moreover, flexible electrode designs could potentially adapt better to the varying anatomical structures of users, improving signal consistency and overall sensing performance across a broader range of individuals.

### 8.2 Data Collection Methods

While our current approach for detecting finger contact and pinch force - using an FSR sensor mounted on the finger - is adapted from

prior research [32], this setup inherently constrains the potential for fully autonomous pinch force estimation. Moreover, our data collection procedures did not rigorously address some interaction scenarios, such as conditions involving significant arm or hand sweating, or interactions involving other limbs or body parts. These may introduce additional noise or variability into impedance measurements, potentially impacting classification accuracy or estimation reliability. For future work, we will explore other non-contact based data labeling approaches, and conduct more extensive user studies to capture diverse environmental and interactive conditions.

### 8.3 Model Generalizability

Our pinch force regressor struggled with generalizing to new users. Results demonstrate that while the predicted force patterns align with the ground truth (i.e., peaks and dips), the values fall within a different range. This suggests that while our regressor can identify pinch force patterns, it limits in accommodating the significant individual differences in body structure and pinching strength. In this work, we improve the generalizability of our models by few-shot learning. Future work can explore a physical calibrator to adjust for these differences across users, improving the model's adaptability, as well as one-shot learning through better representation learning and fine tuning. Additionally, we will investigate data augmentation techniques to generate a diverse set of simulated electrical impedance data in a low-cost and scalable manner, aiming to build a more robust model for both micro-gesture recognition and force estimation. In addition, based on our experiment, the EI-Lite is quite robust to forearm movement, likely because the relative electrode-to-muscle/tendon position stays the same as long as the electrodes are in good contact with skin. However, it can be affected by large wrist rotations, we envision to resolve this in future work by integrating gyroscope reading (e.g. from smart watches) to include wrist orientation information in the model.

### 8.4 Integration with Commercial Smartwatches

EI-Lite's lightweight, four-electrode design makes it highly suitable for integration with commercial smartwatches. Unlike prior systems that often require bulky forearm instrumentation, our configuration can be embedded directly into the smartwatch form factor. For example, two electrodes can be integrated into the watch body on the dorsal wrist side, while the other two can be embedded into the strap or buckle underneath the wrist—maintaining a familiar and unobtrusive design. The electrode size (ca. 1cm in diameter) in our prototype is selected based on the current smartwatch case size (35mm-45mm) for fitting 2 electrodes + spacing (1cm) between. It's also worth noticing that with the current electrode design, only the bottom 1/3 (ca. 3.3mm) of the electrode is contacting the skin, the top 2/3 height can be removed when integrating into wearables. This arrangement enables full 4-terminal impedance sensing without additional accessories, while preserving comfort and wearability. It also opens opportunities for multimodal sensing by combining impedance signals with onboard IMUs, PPG, or haptics. Such integration could expand existing gesture features (e.g., pinch, double pinch) with richer inputs like continuous pinch force or multi-finger gestures, supporting AR/VR and assistive interactions.

## 9 Conclusion

In this paper, we present EI-Lite, a lightweight, wrist-worn electrical impedance sensing device designed for micro-gesture recognition and continuous pinch force estimation. Through an ablation study on electrode placement with 13 users, we optimize the device architecture and validate its performance by capturing data from 15 participants on six common micro-gestures (plus idle state), and index finger pinch forces. Our machine learning models demonstrate high accuracy in recognizing micro-gesture events (96.33%) and achieve precise pinch force estimation, with a mean-squared-error (MSE) of 0.3071 (or mean-force-variance of 0.55 Newtons). We implemented three application examples in AR/VR, gaming, and assistive technologies, to demonstrate EI-Lite's real-world applicability. These results highlight EI-Lite's potential for enhancing HCI applications by providing an intuitive and discreet solution for subtle finger and hand interactions.

## Acknowledgments

We thank the Google PD Labs for their help with early wristband design prototyping development, especially Whitney Bai and Seth. We thank the Googler Initiated Grant and the MIT EECS Transformative Research Fund for their generous support for this research.

## References

- [1] Apple. 2023. Apple Watch double tap gesture now available with watchOS 10.1. Apple Newsroom. <https://www.apple.com/newsroom/2023/10/apple-watch-double-tap-gesture-now-available-with-watchos-10-1/>
- [2] Vincent Becker, Pietro Oldrati, Liliana Barrios, and Gábor Sörös. 2018. Touchsense: classifying finger touches and measuring their force with an electromyography armband. In *Proceedings of the 2018 ACM International Symposium on Wearable Computers* (Singapore, Singapore) (ISWC '18). Association for Computing Machinery, New York, NY, USA, 1–8. <https://doi.org/10.1145/3267242.3267250>
- [3] Edwin Chan, Teddy Seyed, Wolfgang Stuerzlinger, Xing-Dong Yang, and Frank Maurer. 2016. User elicitation on single-hand microgestures. In *Proceedings of the 2016 CHI Conference on Human Factors in Computing Systems*. 3403–3414.
- [4] Liwei Chan, Yi-Ling Chen, Chi-Hao Hsieh, Rong-Hao Liang, and Bing-Yu Chen. 2015. Cyclopsring: Enabling whole-hand and context-aware interactions through a fisheye ring. In *Proceedings of the 28th Annual ACM Symposium on User Interface Software & Technology*. 549–556.
- [5] Victor Chen, Xuhai Xu, Richard Li, Yuanchun Shi, Shwetak Patel, and Yuntao Wang. 2021. Understanding the design space of mouth microgestures. In *Proceedings of the 2021 ACM Designing Interactive Systems Conference*. 1068–1081.
- [6] Weihai Chen, Mingxing Lyu, Xilun Ding, Jianhua Wang, and Jianbin Zhang. 2023. Electromyography-controlled lower extremity exoskeleton to provide wearers flexibility in walking. *Biomedical Signal Processing and Control* 79 (2023), 104096. <https://doi.org/10.1016/j.bspc.2022.104096>
- [7] Vladimir A Cherepenin, Alexander Y Karpov, Alexander V Korjenevsky, Valdimir N Kornienko, Yury S Kultiasov, Mikhail B Ochapkin, Olga V Trochanova, and J David Meister. 2002. Three-dimensional EIT imaging of breast tissues: system design and clinical testing. *IEEE transactions on medical imaging* 21, 6 (2002), 662–667.
- [8] Changmok Choi, Suncheol Kwon, Wonil Park, Hae dong Lee, and Jung Kim. 2010. Real-time pinch force estimation by surface electromyography using an artificial neural network. *Medical Engineering & Physics* 32, 5 (2010), 429–436. <https://doi.org/10.1016/j.medengphy.2010.04.004>
- [9] Ana Cisnal, Javier Pérez-Turiel, Juan-Carlos Fraile, David Sierra, and Eusebio de la Fuente. 2021. RobHand: A Hand Exoskeleton With Real-Time EMG-Driven Embedded Control. Quantifying Hand Gesture Recognition Delays for Bilateral Rehabilitation. *IEEE Access* 9 (2021), 137809–137823. <https://doi.org/10.1109/ACCESS.2021.3118281>
- [10] Nathan Devrio and Chris Harrison. 2022. DiscoBand: Multiview Depth-Sensing Smartwatch Strap for Hand, Body and Environment Tracking. In *Proceedings of the 35th Annual ACM Symposium on User Interface Software and Technology*. 1–13.
- [11] Jörg Eschweiler, Jianzhang Li, Valentin Quack, Björn Rath, Alice Baroncini, Frank Hildebrand, and Filippo Migliorini. 2022. Anatomy, biomechanics, and loads of the wrist joint. *Life* 12, 2 (2022), 188.
- [12] Jun Gong, Yang Zhang, Xia Zhou, and Xing-Dong Yang. 2017. Pyro: Thumb-tip gesture recognition using pyroelectric infrared sensing. In *Proceedings of the 30th Annual ACM Symposium on User Interface Software and Technology*. 553–563.
- [13] R Harikumar, R Prabu, and S Raghavan. 2013. Electrical impedance tomography (EIT) and its medical applications: A review. *Int. J. Soft Comput. Eng* 3, 4 (2013), 193–198.
- [14] Ross P Henderson and John G Webster. 1978. An impedance camera for spatially specific measurements of the thorax. *IEEE Transactions on Biomedical Engineering* 3 (1978), 250–254.
- [15] David Holder. 2005. *Electrical Impedance Tomography : Methods, History and Applications*. Vol. 32. Institute of Physics. <https://doi.org/10.1118/1.1995712>
- [16] Fang Hu, Peng He, Songlin Xu, Yin Li, and Cheng Zhang. 2020. FingerTrak: Continuous 3D hand pose tracking by deep learning hand silhouettes captured by miniature thermal cameras on wrist. *Proceedings of the ACM on Interactive, Mobile, Wearable and Ubiquitous Technologies* 4, 2 (2020), 1–24.
- [17] Da-Yuan Huang, Liwei Chan, Shuo Yang, Fan Wang, Rong-Hao Liang, De-Nian Yang, Yi-Ping Hung, and Bing-Yu Chen. 2016. DigitSpace: Designing Thumb-to-Fingers Touch Interfaces for One-Handed and Eyes-Free Interactions. In *Proceedings of the 2016 CHI Conference on Human Factors in Computing Systems* (San Jose, California, USA) (CHI '16). Association for Computing Machinery, New York, NY, USA, 1526–1537. <https://doi.org/10.1145/2858036.2858483>
- [18] Inc. Interlink Electronics. [n. d.]. FSR 400 short. <https://www.interlinkelectronics.com/fsr-400-short>
- [19] Yasha Iravantchi, Yang Zhang, Evi Bernitsas, Mayank Goel, and Chris Harrison. 2019. Interferi: Gesture sensing using on-body acoustic interferometry. In *Proceedings of the 2019 CHI Conference on Human Factors in Computing Systems*. 1–13.
- [20] Wolf Kienzle, Eric Whitmire, Chris Rittaler, and Hrvoje Benko. 2021. Electroring: Subtle pinch and touch detection with a ring. In *Proceedings of the 2021 CHI Conference on Human Factors in Computing Systems*. 1–12.
- [21] Daehwa Kim and Chris Harrison. 2022. EtherPose: Continuous hand pose tracking with wrist-worn antenna impedance characteristic sensing. In *Proceedings of the 35th Annual ACM Symposium on User Interface Software and Technology*. 1–12.
- [22] David Kim, Otmar Hilliges, Shahram Izadi, Alex D Butler, Jiawen Chen, Jason Oikonomidis, and Patrick Olivier. 2012. Digits: freehand 3D interactions anywhere using a wrist-worn gloveless sensor. In *Proceedings of the 25th annual ACM symposium on User interface software and technology*. 167–176.
- [23] Kenrick Kin, Chengde Wan, Ken Koh, Andrei Marin, Necati Cihan Camgöz, Yubo Zhang, Yujun Cai, Fedor Kovalev, Moshe Ben-Zacharia, Shannon Hoople, et al. 2024. STMIG: A Machine Learning Microgesture Recognition System for Supporting Thumb-Based VR/AR Input. In *Proceedings of the CHI Conference on Human Factors in Computing Systems*. 1–15.
- [24] Alexander Kyu, Hongyu Mao, Junyi Zhu, Mayank Goel, and Karan Ahuja. 2024. EITPose: Wearable and Practical Electrical Impedance Tomography for Continuous Hand Pose Estimation. In *Proceedings of the CHI Conference on Human Factors in Computing Systems*. 1–10.
- [25] Ctrl labs at Reality Labs, David Sussillo, Patrick Kaifosh, and Thomas Reardon. 2024. A generic noninvasive neuromotor interface for human-computer interaction. *bioRxiv* (2024), 2024–02.
- [26] Gierad Laput, Robert Xiao, and Chris Harrison. 2016. Viband: High-fidelity bio-acoustic sensing using commodity smartwatch accelerometers. In *Proceedings of the 29th Annual Symposium on User Interface Software and Technology*. 321–333.
- [27] Guangchuan Li, David Rempel, Yue Liu, Weitao Song, and Carisa Harris Adamson. 2021. Design of 3d microgestures for commands in virtual reality or augmented reality. *Applied Sciences* 11, 14 (2021), 6375.
- [28] Chen Liang, Chun Yu, Yue Qin, Yuntao Wang, and Yuanchun Shi. 2021. DualRing: Enabling subtle and expressive hand interaction with dual IMU rings. *Proceedings of the ACM on Interactive, Mobile, Wearable and Ubiquitous Technologies* 5, 3 (2021), 1–27.
- [29] Yi Liu, Min Peng, Mohammad Rafiq Swash, Tong Chen, Rui Qin, and Hongying Meng. 2021. Holoscopic 3D microgesture recognition by deep neural network model based on viewpoint images and decision fusion. *IEEE Transactions on Human-Machine Systems* 51, 2 (2021), 162–171.
- [30] Yiming Liu, Chunki Yu, Zhen Song, Ya Huang, Kuanming Yao, Tszhung Wong, Jingken Zhou, Ling Zhao, Xingcan Huang, Sina Khazaee Nejad, Mengge Wu, Dengfeng Li, Jiahui He, Xu Guo, Junsheng Yu, Xue Feng, Zhaoqian Xie, and Xinge Yu. 2022. Electronic skin as wireless human-machine interfaces for robotic VR. *Science Advances* 8, 2 (2022), eabl6700. <https://doi.org/10.1126/sciadv.abl6700> arXiv:<https://www.science.org/doi/pdf/10.1126/sciadv.abl6700>
- [31] Yilin Liu, Shijie Zhang, and Mahanth Gowda. 2021. NeuroPose: 3D hand pose tracking using EMG wearables. In *Proceedings of the Web Conference 2021*. 1471–1482.
- [32] Vimal Mollyn and Chris Harrison. 2024. EgoTouch: On-Body Touch Input Using AR/VR Headset Cameras. In *Proceedings of the 37th Annual ACM Symposium on User Interface Software and Technology* (Pittsburgh, PA, USA) (UIST '24). Association for Computing Machinery, New York, NY, USA, Article 69, 11 pages. <https://doi.org/10.1145/3654777.3676455>
- [33] Viet Nguyen, Siddharth Rupavatharam, Luyang Liu, Richard Howard, and Marco Gruteser. 2019. HandSense: capacitive coupling-based dynamic, micro finger

- gesture recognition. In *Proceedings of the 17th Conference on Embedded Networked Sensor Systems*. 285–297.
- [34] Alex Olwal, Thad Starner, and Gowa Mainini. 2020. E-Textile microinteractions: Augmenting twist with flick, slide and grasp gestures for soft electronics. In *Proceedings of the 2020 CHI Conference on Human Factors in Computing Systems*. 1–13.
- [35] Min Peng, Chongyang Wang, and Tong Chen. 2018. Attention based residual network for micro-gesture recognition. In *2018 13th IEEE International Conference on Automatic Face & Gesture Recognition (FG 2018)*. IEEE, 790–794.
- [36] A Romsauerova, A McEwan, Lior Horesh, R Yerworth, RH Bayford, and David S Holder. 2006. Multi-frequency electrical impedance tomography (EIT) of the adult human head: initial findings in brain tumours, arteriovenous malformations and chronic stroke, development of an analysis method and calibration. *Physiological measurement* 27, 5 (2006), S147.
- [37] AS Sadun, J Jalani, and JA Sukor. 2016. Force Sensing Resistor (FSR): a brief overview and the low-cost sensor for active compliance control. In *First international workshop on pattern recognition*, Vol. 10011. SPIE, 222–226.
- [38] Samsung. 2023. More Than a Gesture: How Galaxy Watch’s Universal Gestures Feature Enhances Accessibility. Samsung Global Newsroom. <https://news.samsung.com/global/more-than-a-gesture-how-galaxy-watches-universal-gestures-feature-enhances-accessibility>
- [39] Munehiko Sato, Rohan S. Puri, Alex Olwal, Yosuke Ushigome, Lukas Franciszkiewicz, Deepak Chandra, Ivan Poupyrev, and Ramesh Raskar. 2017. *Zensei: Embedded, Multi-Electrode Bioimpedance Sensing for Implicit, Ubiquitous User Recognition*. Association for Computing Machinery, New York, NY, USA, 3972–3985. <https://doi.org/10.1145/3025453.3025536>
- [40] Martin Schmitz, Sebastian Günther, Dominik Schön, and Florian Müller. 2022. Squeezey-Feely: Investigating Lateral Thumb-Index Pinching as an Input Modality. In *Proceedings of the 2022 CHI Conference on Human Factors in Computing Systems* (New Orleans, LA, USA) (CHI ’22). Association for Computing Machinery, New York, NY, USA, Article 61, 15 pages. <https://doi.org/10.1145/3491102.3501981>
- [41] Adwait Sharma, Christina Salchow-Hömmen, Vimal Suresh Mollny, Aditya Shekhar Nittala, Michael A Hedderich, Marion Koelle, Thomas Seel, and Jürgen Steinle. 2023. SparseIMU: Computational design of sparse IMU layouts for sensing fine-grained finger microgestures. *ACM Transactions on Computer-Human Interaction* 30, 3 (2023), 1–40.
- [42] Yisheng Song, Ting Wang, Subrota K Mondal, and Jyoti Prakash Sahoo. 2022. A Comprehensive Survey of Few-shot Learning: Evolution, Applications, Challenges, and Opportunities. arXiv:2205.06743 [cs.LG]. <https://arxiv.org/abs/2205.06743>
- [43] Scott Stein. 2024. I Wore Meta’s Orion AR Glasses: A Wireless Taste of a Neural Future. CNET. <https://www.cnet.com/tech/computing/i-wore-metas-orion-ar-glasses-a-wireless-taste-of-a-neural-future/>
- [44] Radu-Daniel Vatavu and Laura-Bianca Bilius. 2021. GestuRING: A Web-based Tool for Designing Gesture Input with Rings, Ring-Like, and Ring-Ready Devices. In *The 34th Annual ACM Symposium on User Interface Software and Technology* (Virtual Event, USA) (UIST ’21). Association for Computing Machinery, New York, NY, USA, 710–723. <https://doi.org/10.1145/3472749.3474780>
- [45] Radu-Daniel Vatavu and Ovidiu-Ciprian Ungurean. 2022. Understanding gesture input articulation with upper-body wearables for users with upper-body motor impairments. In *Proceedings of the 2022 CHI Conference on Human Factors in Computing Systems*. 1–16.
- [46] Tijana Vuletić, Alex Duffy, Laura Hay, Chris McTeague, Gerard Campbell, and Madeleine Grealy. 2019. Systematic literature review of hand gestures used in human computer interaction interfaces. *International Journal of Human-Computer Studies* 129 (2019), 74–94.
- [47] Anandghan Waghmare, Youssef Ben Taleb, Ishan Chatterjee, Arjun Narendra, and Shwetak Patel. 2023. Z-Ring: Single-Point Bio-Impedance Sensing for Gesture, Touch, Object and User Recognition. In *Proceedings of the 2023 CHI Conference on Human Factors in Computing Systems*. 1–18.
- [48] Anandghan Waghmare, Roger Boldu, Eric Whitmire, and Wolf Kienzle. 2023. OptiRing: Low-Resolution Optical Sensing for Subtle Thumb-to-Index Micro-Interactions. In *Proceedings of the 2023 ACM Symposium on Spatial User Interaction* (Sydney, NSW, Australia) (SUI ’23). Association for Computing Machinery, New York, NY, USA, Article 8, 13 pages. <https://doi.org/10.1145/3607822.3614538>
- [49] Anandghan Waghmare, Ishan Chatterjee, and Shwetak Patel. 2023. Z-Pose: Continuous 3D Hand Pose Tracking Using Single-Point Bio-Impedance Sensing on a Ring. In *Proceedings of the 2nd Workshop on Smart Wearable Systems and Applications* (Madrid, Spain) (SmartWear ’23). Association for Computing Machinery, New York, NY, USA, 1–6. <https://doi.org/10.1145/3615592.3616851>
- [50] Cong Wang, Deepak Vungarala, Kevin Navarro, Neel Adwani, and Tao Han. 2023. The Pinch Sensor: An Input Device for In-Hand Manipulation with the Index Finger and Thumb. In *2023 IEEE/ASME International Conference on Advanced Intelligent Mechatronics (AIM)*. 822–827. <https://doi.org/10.1109/AIM46323.2023.10196268>
- [51] Nana Wang, Jianwei Niu, Xuefeng Liu, Dongqin Yu, Guogang Zhu, Xinghao Wu, Mingliang Xu, and Hao Su. 2024. BeyondVision: An EMG-driven Micro Hand Gesture Recognition Based on Dynamic Segmentation. In *Proceedings of the Thirty-Third International Joint Conference on Artificial Intelligence, IJCAI-24*, Kate Larson (Ed.), International Joint Conferences on Artificial Intelligence Organization, 6044–6052. <https://doi.org/10.24963/ijcai.2024/668> Main Track.
- [52] Martin Weigel, Tong Lu, Gilles Bailly, Antti Oulasvirta, Carmel Majidi, and Jürgen Steinle. 2015. iSkin: Flexible, Stretchable and Visually Customizable On-Body Touch Sensors for Mobile Computing. In *Proceedings of the 33rd Annual ACM Conference on Human Factors in Computing Systems* (Seoul, Republic of Korea) (CHI ’15). Association for Computing Machinery, New York, NY, USA, 2991–3000. <https://doi.org/10.1145/2702123.2702391>
- [53] Katrin Wolf. 2016. Microgestures—enabling gesture input with busy hands. *Peripheral Interaction: Challenges and Opportunities for HCI in the Periphery of Attention* (2016), 95–116.
- [54] Chenhan Xu, Bing Zhou, Gurunandan Krishnan, and Shree Nayar. 2023. AoFinger: Hands-free fine-grained finger gesture recognition via acoustic-optic sensor fusing. In *Proceedings of the 2023 CHI Conference on Human Factors in Computing Systems*. 1–14.
- [55] Xuhai Xu, Jun Gong, Carolina Brum, Lilian Liang, Bongsoo Suh, Shivam Kumar Gupta, Yash Agarwal, Laurence Lindsey, Runchang Kang, Behrooz Shahsavari, Tu Nguyen, Heriberto Nieto, Scott E Hudson, Charlie Maalouf, Jax Seyed Mousavi, and Gierad Laput. 2022. Enabling Hand Gesture Customization on Wrist-Worn Devices. In *Proceedings of the 2022 CHI Conference on Human Factors in Computing Systems* (New Orleans, LA, USA) (CHI ’22). Association for Computing Machinery, New York, NY, USA, Article 496, 19 pages. <https://doi.org/10.1145/3491102.3501904>
- [56] Hui-Shyong Yeo, Erwin Wu, Juyoung Lee, Aaron Quigley, and Hideki Koike. 2019. Opisthenar: Hand poses and finger tapping recognition by observing back of hand using embedded wrist camera. In *Proceedings of the 32nd Annual ACM Symposium on User Interface Software and Technology*. 963–971.
- [57] Jinyang Yu, Chentao Li, Jianjiang Feng, and Jie Zhou. 2025. 3D Touch Force Estimation from Capacitive Images. In *Proceedings of the 30th International Conference on Intelligent User Interfaces (IUI ’25)*. Association for Computing Machinery, New York, NY, USA, 1–17. <https://doi.org/10.1145/3708359.3712123>
- [58] Wenzhen Yuan, Siyuany Dong, and Edward H. Adelson. 2017. GelSight: High-Resolution Robot Tactile Sensors for Estimating Geometry and Force. *Sensors* 17, 12 (2017). <https://doi.org/10.3390/s17122762>
- [59] Yang Zhang and Chris Harrison. 2015. Tomo: Wearable, Low-Cost Electrical Impedance Tomography for Hand Gesture Recognition. In *Proceedings of the 28th Annual ACM Symposium on User Interface Software & Technology* (Charlotte, NC, USA) (UIST ’15). Association for Computing Machinery, New York, NY, USA, 167–173. <https://doi.org/10.1145/2807442.2807480>
- [60] Yang Zhang, Gierad Laput, and Chris Harrison. 2017. Electrick: Low-Cost Touch Sensing Using Electric Field Tomography. In *Proceedings of the 2017 CHI Conference on Human Factors in Computing Systems* (Denver, Colorado, USA) (CHI ’17). Association for Computing Machinery, New York, NY, USA, 1–14. <https://doi.org/10.1145/3025453.3025842>
- [61] Yang Zhang, Robert Xiao, and Chris Harrison. 2016. Advancing Hand Gesture Recognition with High Resolution Electrical Impedance Tomography. In *Proceedings of the 29th Annual Symposium on User Interface Software and Technology* (Tokyo, Japan) (UIST ’16). Association for Computing Machinery, New York, NY, USA, 843–850. <https://doi.org/10.1145/2984511.2984574>
- [62] Junyi Zhu, Young Joong Lee, Yiyue Luo, Tianyu Xu, Chao Liu, Daniela Rus, Stefanie Mueller, and Wojciech Matusik. 2024. Liquids Identification and Manipulation via Digitally Fabricated Impedance Sensors. In *2024 IEEE International Conference on Robotics and Automation (ICRA)*. IEEE, 18164–18171.
- [63] Junyi Zhu, Yuxuan Lei, Aashini Shah, Gila Schein, Hamid Ghaednia, Joseph Schwab, Casper Harteveld, and Stefanie Mueller. 2022. MuscleRehab: Improving unsupervised physical rehabilitation by monitoring and visualizing muscle engagement. In *Proceedings of the 35th Annual ACM Symposium on User Interface Software and Technology*. 1–14.
- [64] Junyi Zhu, Jackson Snowden, Joshua Verdejo, Emily Chen, Paul Zhang, Hamid Ghaednia, Joseph H. Schwab, and Stefanie Mueller. 2021. EIT-kit: An Electrical Impedance Tomography Toolkit for Health and Motion Sensing. In *Proceedings of the 34th Annual ACM Symposium on User Interface Software and Technology*. <https://doi.org/10.1145/3472749.3474758>
- [65] Y Zou and Z Guo. 2003. A review of electrical impedance techniques for breast cancer detection. *Medical engineering & physics* 25, 2 (2003), 79–90.